Accepted Manuscript

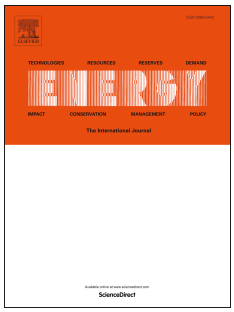

Projections of wind energy resources in the Caribbean for the 21st century

X. Costoya, M. deCastro, F. Santos, M.C. Sousa, M. Gómez-Gesteira

PII: S0360-5442(19)30754-6

DOI: https://doi.org/10.1016/j.energy.2019.04.121

Reference: EGY 15150

To appear in: *Energy*

Received Date: 17 July 2018

Revised Date: 3 April 2019

Accepted Date: 19 April 2019

Please cite this article as: Costoya X, deCastro M, Santos F, Sousa MC, Gómez-Gesteira M, Projections of wind energy resources in the Caribbean for the 21st century, *Energy* (2019), doi: https://doi.org/10.1016/j.energy.2019.04.121.

Projections of wind energy resources in the Caribbean for the 21st century

X. Costoya[1,2*], M. deCastro[1], F. Santos[1,2], M. C. Sousa[2], M. Gómez-Gesteira[1]

[1] Environmental PHYsics LABoratory (EPHYSLAB), Facultade de Ciencias, Universidade de Vigo, 32004 Ourense, Spain.

[2] CESAM – Department of Physics, University of Aveiro, Campus Universitário de Santiago, Aveiro, Portugal

*Corresponding author. Tel.: +34 988387255. Fax: +34 988387227

E-mail address: jorge.costoya@ua.pt

Abstract

The Caribbean has suitable conditions for a significant wind energy development, which makes a good planning for the future renewable energy mix essential. The impact of climate change on Caribbean wind power has been analyzed by means of an ensemble of CORDEX regional climate models (RCMs) under the RCP8.5 warming scenario. The offshore wind energy resource was classified for the historical period and for the future considering wind energy factors, environmental risk factors and cost factors whose weights were estimated by a Delphi method.

Future projections show a maximum annual wind increase, ~0.4 ms^{-1} (8%), in most of the Caribbean, except in the Yucatán Basin. This increment occurs mainly during the wet season, ~0.5 ms^{-1} (~10%), associated with changes in the extension of the North Atlantic Subtropical High, which will strengthen the Caribbean low-level jet. Additionally, the moderate wind increase, ~0.2 ms^{-1} (~4%), projected during the dry season is restricted to the southeastern coast and it is associated with an increment in the land-ocean temperature difference (~1°C), which will intensify local easterly winds. The low-level jet region was classified as the richest wind energy resource in the Caribbean for the future with a larger extension compared to the historical period.

Keywords: renewable energy; wind farms; climate change; CORDEX; Caribbean, Delphi method.

1. Introduction

The Caribbean has very good conditions to a significant increase in renewable energy development due to its location close to the equator (almost uninterrupted sunlight) and the influence of the northeasterly trade winds. The North Atlantic Subtropical High (NASH), located over the Atlantic Ocean, produces strong northeasterly trade winds over the eastern Caribbean. In fact, the Caribbean Sea has wind energy values above the average compared to the rest of the subtropical Atlantic Ocean according to previous studies dealing with wind power density worldwide [1-2]. Most Caribbean countries lie between 10°N and 30°N and are influenced by the trade wind belt (between 5°N and 30°N). Additionally, most of these countries have a high dependence on fossil fuel imports at high prices (only Venezuela and Trinidad and Tobago have enough oil and gas reserves for local consumption and export). The average cost of electricity in the Caribbean is very high (US $0.31/kWh) compared to the USA (US $0.12/kWh) and Canada (US $0.10/kWh) due to fuel import charges [3]. The development of renewable energy would enable a more sustainable energy supply in the future and help in the production of fresh water, as well as reducing carbon dioxide emissions of Caribbean countries, whose economy is based mainly on tourism [4] and agriculture. For these reasons, Caribbean countries are good candidates for the use of a renewable energy mix. In many of these countries, this mix is based mainly on solar (photovoltaic panels) and wind energy (wind turbines). The long dry season and the lack of volcanic zones and large rivers preclude the possibility of developing other forms of renewable energy such as geothermal and hydroelectric power.

In recent decades, the development of wind technologies has gained more strength because they are less costly than photovoltaic technologies. The cost of equipment and maintenance of wind turbines has fallen at the same time as their efficiency and availability have improved, with larger turbines available for intercepting higher wind speeds. Large contemporary wind turbines make electricity generation from wind farms cost-competitive with electricity from fossil fuels [5]. Some Caribbean islands, notably Cuba, Curaçao, Jamaica, Martinique and Guadalupe, have already implemented wind farms [6]. For the development of wind energy projects, comprehensive knowledge and quantification of near-surface wind climate and wind resources provide an idea of the wind power available in the region. The first analysis of the wind energy resource in the Caribbean and Central America was carried out using in-situ data [7]. Although this study was mainly focused in

land areas with a low spatial resolution, the authors classified the Caribbean marine areas into different wind power categories using data from ships. They found that most of the Caribbean Sea has an annual average wind power >200 W m^{-2}, which is beneficial for most applications related to wind energy exploitation. More recently, wind power availability in the Caribbean was analyzed by means of reanalysis data [8], which assimilated 10 m winds from land stations, buoys, ships and satellites from 1979 to 2010. The annual wind resource map shows the Caribbean low level jet (CLLJ) region as having the highest wind power resource (400–600 W m^{-2}) followed by the Netherland Antilles as an excellent region (300–400 W m^{-2}) and the Greater Antilles and the Bahamas as a good wind resource (200–300 Wm^{-2}). In addition, wind power is shown to be greater during the dry season (350 Wm^{-2}) than during the wet season (247–290 Wm^{-2}), where the wet season covers the period May–November and the dry season December–April. On a more regional scale, wind characteristics were also analyzed with emphasis on the suitability of the climate for wind technology applications in Puerto Rico Island [9], the Yucatán Peninsula [10], Jamaica Island [11], Barbados Island [12], Grenada Island [13] and Trinidad and Tobago Island [5] using wind data from meteorological stations.

Good planning of the future renewable energy mix depends on the impact of climate change on future wind power production. This planning should be founded on reliable climate projections, using high spatial resolution models whose accuracy has been tested and verified against real data. On a regional scale, future wind variations and their geographical distribution will have a direct impact on wind power production, making some regions more suitable than others for installing wind farms. Climate models have been shown to be the most useful tool for simulating and projecting the impact of future climate change on wind circulation patterns [14–23]. These models consider atmospheric chemistry, aerosols and the carbon cycle, and incorporate the interaction between the atmosphere, land-use and vegetation. The Coordinated Regional Climate Downscaling Experiment (CORDEX) is the most recent and largest ensemble of Regional Climate Models (RCMs). This uses as forcing the state-of-the-art Global Climate Models (GCMs) from the Coupled Model Intercomparison Project Phase 5 (CMIP 5) for different regional climate-change scenarios. The CORDEX project has more ensemble members, emission scenarios and higher spatial resolution to better reproduce the topography, land use and

smaller-scale meteorological processes than its predecessors, the PRUDENCE and ENSEMBLES projects. Even so, models are always simplified representations of the earth's climate system. Climate models have some limitations because not all temporal and spatial scales can be resolved and not all processes within the Earth's system are yet fully understood, and thus are not directly quantifiable in explicit terms (e.g., turbulent exchanges in stable conditions, or aerosol life cycles). Additionally, the results depend on the climate model configuration (surface characteristics, the number of vertical levels, parameterizations, the numerical scheme used to solve the equations…). However, in general, according to the EURO-CORDEX Guidelines [24], climate models are becoming able to simulate the state and trends of the climate for longer time periods and larger regions than previously. Special care has to be taken if regional climate models are used to study events occurring at small temporal and spatial scales, such as at a particular location (i.e., a single grid box) or a short time period (e.g. single storm events).

Although the impact of climate change on mean wind, wind power and wind extremes has been studied both at global and regional scales worldwide for the 21st century [14–23], there is a lack of information about the influence of climate change on wind power resources in the Caribbean. Future solar and wind energy spatial patterns were simulated for Puerto Rico by means of the parallel climate model (PCM) coupled with the regional atmospheric model (RAMS) [25]. Their numerical results indicate a slight decrease in the net surface solar radiation in the Caribbean Basin, being more pronounced in the western part, for the period 2041–2055 compared to the 1996–2010 period. They also projected an increase in easterly winds in 2070–2098, especially around the coast. Differences in wind speed were also analyzed, but in that case by means of a statistical downscaling of only one GCM (GFDL CM2.1) [26]. Wind speeds for two different emission scenarios, a pre-industrial scenario and a scenario with more than triple the pre-industrial levels, were compared for the month of April (the transition month between dry and wet season) from 2069 to 2079. A slight increase in wind power was projected for most of the Caribbean Sea.

However, the offshore wind energy exploitation depends not only on the characterization of the regional wind regime but also on a series of factors related to environmental risk and cost as previously stated by [2]. In this previous study, a Delphi method was developed to

classify the worldwide offshore wind energy taking into account wind energy factors (wind power density, WPD, effective wind speed occurrence, EWSO, rich level occurrence, RLO), environmental risk factors (extreme wind speed, EWS, coefficient of variation, Cv and monthly variability index, Mv,) and cost factors (water depth, WD, and distance to coast, DC) to categorize the global offshore wind energy resource. According to historical records, they classified the offshore wind energy resource of the Caribbean as better than good following their new wind energy classification [2].

The aim of the present study is to analyze future wind resources projections in the Caribbean for the 21st century both annually and seasonally. The analysis was carried out by means of a high spatial resolution ensemble of CORDEX RCMs under the greenhouse gas scenario RCP 8.5 for three future time periods: near future (2019–2045), mid-future (2046–2072) and far future (2073–2099). The capability of the RCMs to reproduce real wind data measured by *in situ* buoys was previously tested by means of the overlap between measured and modeled probability distribution functions from 2009 to 2016. Additionally, a method similar to the one described in [2] was applied to classify the future offshore wind energy resource in the Caribbean Sea taking into account wind energy factors, environmental risk factors and cost factors.

2. Data and methods

2.1. Data

The analysis of future wind and wind power projections for the Caribbean was developed by means of seven RCMs simulations carried out within the framework of CORDEX project (http://www.cordex.org) at a spatial resolution of 0.44º x 0.44º. The regional simulations were carried out by means of a multi-model-ensemble with one RCM (RCA4) forced by seven GCMs under the RCP8.5 future emission scenario (Table 1). The use of the largest possible model ensemble, both for evaluation and application of RCMs, is recommended to achieve robust results. As mentioned above, RCP 8.5 represents very high greenhouse gas emission leading to 8.5 Wm-² radiative forcing, which is projected to continue rising even after 2100. For further information on future regional climate

projections from the CORDEX project (climate scenarios, the limits of climate modeling, evaluation of the RCM simulations and how to interpret and adjust model biases, among others) the reader is referred to [24].

Daily wind speed data at 10 m height, monthly surface air temperatures and sea level atmospheric pressures were considered in the present study. Sea level pressure was used to analyze the position of the NASH for the 21st century; surface air temperature was used to analyze the difference between land and ocean temperatures (see locations in Figure 1).

Three different periods were considered for future projections: near future (2019–2045), mid-future (2046–2072) and far future (2073–2099). Far future projections are considered to be merely theoretical, because the typical lifetime of wind turbines is considerably shorter; nevertheless, it may be assumed that the lifetime of a wind farm is much longer than the life of individual turbines due to the frequent replacement and updating of wind turbines in existing wind farms. Historical simulations for 1976–2005 were also considered for comparison purposes.

The capability of RCMs to reproduce *in situ* wind behavior was evaluated from hourly wind data obtained from five marine buoys distributed along the Caribbean Sea, deployed by the National Data Buoy Center (http://www.ndbc.noaa.gov) from 2009 to 2016 (Figure 1, numbers). Buoys sample wind speed and direction at a height of 4 m above sea level and their coordinates are described in Table 2. It can be seen that at least one buoy was present in each basin of the area under scope. Considering this fact, a first wind speed characterization was carried out by representing, the Weibull distribution for each buoy (Figure 2), which is the most widely method used to characterize wind speed [27]. Weibull distribution is a two-parameter probability density function that, in this case, represent the frequency distribution at 0.1 ms^{-1} wind speed range for the whole period available at each buoy. It depends on two parameters also shown in Figure 2: the shape parameter (k) and the scale parameter (c) which is proportional to the average wind speed.

2.2. Methods

2.2.1. Offshore wind data extrapolation

Wind data from buoys and from the CORDEX project were respectively extrapolated from 4 m and 10 m to 120 m, which is the typical hub height of offshore wind turbines. This is done using methods that account for atmospheric stability, such as Monin-Obukhov theory [28] or the Liu and Tang method [29]. However, the buoys considered in the present study do not collect the necessary measurements of temperature, heat flux and friction velocity to allow correct application of these methods. In addition, the CORDEX project does not contain all the necessary variables for calculating atmospheric stability at each time and pixel. Therefore, wind extrapolation was carried out using a logarithmic wind profile [Eq. (1)] that assumes a neutrally stratified atmosphere [30], following the expression applied in previous studies [22, 31]. This approach was selected as the best option to reach a compromise between availability and low cost for data [32].

$$W_H = W_{ns} \frac{\ln\left(\frac{H}{z_0}\right)}{\ln\left(\frac{H_{ns}}{z_0}\right)} \quad (1)$$

where H is the hub height of the offshore wind turbine; H_{ns} is the height at which near-surface winds are measured (10 m for CORDEX and 4 m for buoys); W_H is the wind speed at the hub height; W_{ns} is the near-surface wind speed; and z_0 is the roughness length. At ocean locations, a value of z_0 = 0.001 m was assumed for open calm sea [33, 34]. Variations of mean wind speed depending on height can be seen in Figure S1 (Supplementary material).

2.2.2. Wind power calculation

The wind power density (WPD) of a turbine depends on air density and wind velocity. It can be calculated according to [35] by the following expression:

$$WPD = \frac{1}{2}\rho_a \mathrm{W_H}^3 \quad (2)$$

where ρ_a is the air density (1.225 kgm^{-3} at 15°C and 1000 hPa).

WPD (in watts m^{-2}) indicates how much energy is available to be converted by a wind turbine at a specific place. So, this variable is the most appropriate to compare different locations before wind farms are installed. WPD does not consider the specific properties of a wind turbine, which agrees with the main purpose of the present study. It is expected that the efficiency and the structural properties of wind turbines (as hub height or rotor diameter) will be improved in the future. For this reason, this study was focused on the energy available in the wind (WPD) and its variation in the future.

2.2.3. Geostrophic winds calculation

Geostrophic wind components resulting from the balance of Coriolis force and pressure gradient force were calculated from the formulas described in [36]. Geostrophic wind calculation, which is based on the monthly surface atmospheric pressure fields, allowed analyzing variations of the NASH over the 21st century.

2.2.4. Multi-model validation

The capacity of a RCM to predict future winds was statistically analyzed in terms of the percentage of overlap (OP) between the measured and modeled probability distribution functions (PDF) using a procedure similar to that in [37], where OP equal to 100% indicates coincident PDFs, thus reproducing in situ data perfectly. This procedure enables comparison of the whole data distribution, ensuring that the main features of the dataset are satisfactorily captured by the model [37].

Future changes in wind speed and power were evaluated as the percentage of change for each future period, calculated from:

$$\% = \frac{\langle V_F \rangle - \langle V_H \rangle}{\langle V_H \rangle} * 100 \quad (3)$$

where $< V_F >$ is the mean value of the wind module or wind power for each future period and $< V_H >$ for the historical period.

The multi-model approach makes possible to determine the significance of the differences calculated following equation 3 by analyzing if an agreement exists between the different models that compound the multi-model. This methodology is called the consensus criterion [22, 38] and it is based on imposing two conditions to determine if a pixel is statistically significant:

1. Wind differences were calculated following equation 4 for each model separately and also for the multi-model mean. The first condition is that at least 70% of all models agreed in the direction of change compared to the direction of change of the multi-model mean, that is, if a pixel has a positive sign in the multi-model mean, at least 70% of the 7 RCMs should also have a positive sign for this pixel.
2. The Mann-Whitney (or Wilcoxon rank sum test) non-parametric test was applied at every pixel, both for each model and for the multi-model mean, because wind speed and wind power are, generally, not normally distributed functions [39]. The Mann-Whitney test cross-checks the null hypothesis that two data samples belong to continuous distributions with equal medians, against the alternative that they do not. A 5% significance level was considered at each grid point. To fulfill the second condition, it was imposed that at least 80% of the models that fulfilled the first condition passed the Mann-Whitney-Wilcoxon test.

2.2.5. Classification off the offshore wind energy resource

A method similar to the one developed by [2] was carried out to classify the future offshore wind energy resource in the Caribbean. This method considers wind energy factors, environmental risk factors and cost factors, all of them necessary for the future wind energy exploitation. The indices that characterizes these three types of factors were taken from [1] and [2].

The wind power density, WPD, is based on the wind power classification developed by NREL [40], where 7 categories were considered depending on the annual average wind speed (Table 3). The frequency of occurrence of effective wind speed, EWSO, means that wind speed was in the range that allows producing wind energy, typically defined as 4-25 ms^{-1}. The rich level occurrence, RLO, was defined as the frequency of energy levels higher than 200 Wm^{-2}.

The stability of wind energy was also taken into account because offshore wind energy storage still reminds a challenge [41]. A stable energy supply throughout the year would improve the conversion efficiency and, therefore, its viability. In order to measure wind stability, two indices were applied, the Coefficient of variation index (C_v) and the Monthly variability index (M_v), calculated as follows:

$$C_v = \frac{S}{\bar{x}}$$

where S is the standard deviation and $\bar{x}$ is the mean value.

$$M_v = \frac{P_{M1} - P_{M12}}{P_{year}}$$

where P_{M1} and P_{M12} is the average WPD calculated at the months with the highest and the lowest mean WPD, respectively; P_{year} is the annual averaged WPD.

Extreme wind speeds, EWS, were also considered because they can highly impact the safety of ocean engineering. Its calculation was based on the Gumbel curve method, for which a return period of 50 years was considered.

Finally, cost factors were considered attending to the water depth (WD) and distance to coast (DC) for each pixel of the area under scope. These are crucial factors for marine engineering and electricity interconnection. For this purpose, the ETOPO bathymetry and the Global Self-consistent, Hierarchical, High-resolution Geography (GSHHG) coastline database were considered.

Because each index has different magnitudes with different units it was necessary to carry out a normalization to integrate all factors in a unique value of wind energy resource. The normalization carried out in the present study is a little different from that applied by [2]

worldwide. In this regional study, all factors were normalized considering five categories with the exception of the WPD parameter, which was normalized following categories from Table 3. Table 4 shows the five ranges of values for each factor. Normalized values are calculated in such way that both positive and negative indicators were converted into positive indicators with the optimal value of 1 and the worse 0.

Once normalized, a weight coefficient was applied to each factor following the Delphi approach developed by [2]. These coefficients, shown in Table 5, were derived from the evaluation of ten experts and engineers in the field of wind energy.

The final value of the wind energy resource was then obtained multiplying the weight coefficient set for the normalized values and classified in seven categories according to Table 6 [2]. Following this classification, an area is considered a rich wind energy resource when the final value is higher than 0.6. This method was applied for historical and future periods with the aim of comparing the spatial distribution of regions with rich wind energy resource currently and in the future.

3. Results and Discussion

3.1. Capability of CORDEX models to reproduce Caribbean wind data

The extent to which CORDEX models can reproduce real wind conditions was analyzed by comparing CORDEX-projected winds with *in situ* data from buoys from 2009 to 2016, calculated by the OP between measured and modeled data. Results are summarized in Table 7.

Overall, the mean overlap percentage for the whole region (M, last row) was similar for all models, ranging from 87.6 ± 6.4% (M7) to 95.5 ± 2.5% (M2). The multi-model mean of the overlap percentage (<OP>M, last column) was found to depend on the location of the buoy, ranging from 89.4 ± 5% (at buoy 4) to 94.8 ± 2% (at buoy 1). Overall, the mean average for all models and buoys was 92.4 ± 4.9%.

In summary, taking into account that the accuracy of all models was similar, subsequent analyses were based on multi-model means, where all models were assigned the same

weight. Multi-model means had lower uncertainties and produced better results than individual models, which minimized individual model bias [42, 43].

3.2. Wind speed and wind power evolution for the 21st century.

Once the capability of CORDEX RCMs to reproduce wind has been assessed for the Caribbean, the impact of climate change on wind for the 21st century was analyzed. Climate models are used to analyze future climate projections, from multi-decadal to centennial time scales. The uncertainty in the simulated temporal evolution of climate may be estimated by adopting a range of ensemble simulation strategies, including the multi-model ensemble. In the present study the analysis of wind speed and wind power evolution for the future was carried out by means of a multi-model ensemble of RCMs for RCP 8.5. The multi-model ensemble simulation method minimizes the modeling uncertainties due to, among other factors, the different parameterizations and the numerical approaches used in each model, and also to the initial conditions of the climate system, as each global model is initialized at a different climate state. Note that these multi-model simulations produce future projections, not forecasts, because the results are obtained only from possible emission scenarios [24]. In the present case, the least favorable greenhouse gas emission scenario for the 21st century was adopted.

3.2.1. Annual wind energy projection

Figure 3 shows the multi-model mean for wind speed (Fig. 3a) and wind power (Fig. 3b) and their standard deviations (Figs. 3c, d) for the period 2019–2099. The highest wind speeds were projected for the Colombian Basin (~14 ms^{-1}). Intense winds speeds (~10 ms^{-1}) were also projected for the Venezuela Basin, with more moderate speeds (~7 ms^{-1}) for the Yucatán Basin. Wind power density followed a similar pattern: highest values in the Colombian Basin (~1500 Wm^{-2}), intense (700 Wm^{-2}) in the Venezuela Basin and moderate (250 Wm^{-2}) in the Yucatán Basin. Low standard deviations for mean wind speed and WPD were obtained for most of the Caribbean (Figs. 3c, d) with the highest values being in the regions where the highest mean wind speed and WPD were projected.

The projected WPD highlighted that regions with high power resources at present (i.e., Caribbean low-level jet region, 400–600 Wm^{-2}, eastern Caribbean 300–400 Wm^{-2} and the Netherland Antilles 200–300 Wm^{-2} [8]) will continue to be potentially important or even more suitable for the installation of wind farms during the 21st century. Annual WPD projected for Colombian and Venezuela basins for the 21st century was higher than WPD projected in other regions also by means of CORDEX. In this way, future WPD around 500 Wm^{-2} were projected in most of the Mediterranean and Black seas [23], where it is expected a wind speed decrease over the 21st century under RCP 8.5. Higher values (800-1200 Wm^{-2}) were projected for the North European Atlantic coast and lower WPD in the South Atlantic area. Along the western Iberian Peninsula, future WPD lower than 400 Wm^{-2} were projected at a height of 90 m [14]. Considering that offshore wind farms are planned in some of these areas, such as the Mediterranean Sea or the Iberian Peninsula ([44]), it can be deducted that Caribbean Sea has a great potential as offshore wind energy resource to be exploit.

Figure 4 shows the multi-model mean of the wind percentage of change for the three future temporal periods with respect to the historical period. Overall, there was a consensus between models in the projection of a higher wind speed in most of the Caribbean in the future. Maximum changes of ~8% were projected in the Colombian Basin and ~4% in the Venezuela Basin for far future (Fig. 4c). The Yucatán Basin is the only region in which reductions were projected with a wind speed decrease of ~6% for the far future.

3.2.2. Seasonal wind energy projection

The Caribbean climate is characterized by two seasons, the dry season from December to April and the wet season from May to November [45]. Figure 5 shows the multi-model of the mean wind calculated for the dry season (Fig.5a) and wet season (Fig. 5b) for 2019–2099. Spatially, the strongest winds were obtained in the Colombia Basin, with values around 14 ms^{-1}. Values were slightly more intense in the dry season (Figure 5a), when winds >10 ms^{-1} were projected for most of the Colombia and Venezuela Basins. Seasonal differences were also projected for the Yucatán Basin, with slightly stronger winds during the dry season (Fig. 5a).

A similar pattern was observed for the multi-model mean of wind power (Figure 6). Projected values were >1,000 Wm^{-2} in the Colombian Basin for both seasons, but occupied a larger area in the dry season (Figure 6a). As for wind speed, projected wind power was also slightly larger in the Yucatán Basin during the dry season (Figure 6a). Future projections of the seasonal wind power coincide with the seasonal wind power measured at present, with larger values in the CLLJ region during the dry season (350 Wm^{-2}) than in the wet season (290–247 Wm^{-2}) [8].

Figure 7 is a multi-model mean of the wind percentage of change for dry season (left-hand column) and wet season (right-hand column). For both seasons, the pattern was similar for the three future periods, although the magnitude of change increased over time. However, the changes were completely dependent on the season. During the dry season, projected winds showed only a moderate increase (around 4%) in the Venezuela Basin. For the rest of the region, a wind decrease was projected being up to >5% in the Guajira region of the Colombian Basin for the far future (Figure 7e). On the other hand, there was a consensus between models for an increase (~ 10%) in projected winds for most areas of the Caribbean Basin during the wet season, especially for the mid- and far future. Only the Yucatán Basin showed a wind decrease (~10%) during the wet season.

The multi-model mean of the percentage of change for seasonal wind power showed a similar pattern to that described for wind speed (Figure 8). Models showed a consensus in a wind power decrease for most of the Caribbean during dry season being more than 20% in the Colombian Basin for far future. In addition, there was also a consensus in a moderate increase (~10%) in the Venezuela Basin for all temporal periods. During the wet season, existed a consensus in a wind power increment in the Colombian and Venezuela Basins and a decrease in the Yucatán Basin for all temporal periods, with a maximum decrease of about -20% projected for the far future.

3.2.3. Dynamical analysis of future changes

Both wind speed and power were projected to be larger during the dry season for the rest of the 21st century. An increment in wind speed and power relative to the historical period

1976–2005 was projected to occur during the wet season over most of the area (except in the Yucatán Basin) for all future time periods. This behavior is associated with the future increase of wind intensity in the southeastern Caribbean region during the wet season. The boreal maximum observed in the CLLJ in July is related to the strengthening and movement of the NASH [46, 47]. Thus, NASH values for the far future and the historical period were compared (Figure 9) during boreal summers (wet season). Figure 9a, b shows the mean atmospheric pressure at sea level for the far future and the historical period, respectively. The comparison indicated negligible strengthening of the NASH center over the rest of the 21st century. In addition, the displacement of the center was also negligible (<0.2° latitude and longitude) and consequently undetectable on the measurement grid (1° × 1°). In spite of the small magnitude of these changes, the shape of the isobar pattern is different, producing important differences in the geostrophic wind module. Figure 9c shows the percentage of change of the geostrophic wind for the Caribbean during the boreal summer (wet season). An increase of about 10% was observed for the southern Caribbean (Figure 9c) as a result of the widening of NASH in the far future, consistent with the percentages of wind change (Figure 7).

The projected increase in wind speed and power were less intense for the dry season than for the wet season and were restricted to a small region in the Venezuela Basin. The increase was associated with incremental differences in surface air temperature for land (blue points, Figure 1) and ocean (red points, Figure 1). A comparison of far future temperature projections with temperatures recorded during the 30-year historical period implied an increase of 1°C in the land-ocean temperature differential by the end of the 21st century. This would cause intensification of local easterly winds [47]. Within a framework of global warming, terrestrial warming may occur more rapidly than oceanic warming during the rest of this century, resulting in a strengthening of the southeastern CLLJ.

3.2.4. Classification of the offshore wind energy resource in the Caribbean

The classification of the offshore wind energy resource in the Caribbean, analyzed taking into account wind energy, environmental risk factors and cost factors, is shown in Figure 10 both for the historical period (a) and for near (b), mid (c) and far (d) future. This

classification was carried out according to the criterion specified in Table 6. This criterion was established after calculating the value of wind energy resource multiplying the normalized values (Table 4) by the weighting coefficients (Table 5).

During the historical period, most of the Caribbean Sea was classified in a category higher than 4, which means that the wind resource is better than good, with some particular areas close to Colombia and Venezuela coasts reaching higher values (classes 6 and 7). However, some coastal areas of Central America and the Yucatan Basin showed to have a poor wind energy resource. Overall, the historical wind energy classification obtained for the Caribbean is in good agreement with previous studies [1,2]. As for the future wind energy classification (Figures 10 b, c, d), the Caribbean regions classified as outstanding (class 6) will extend progressively in the future. The richest area in the future will remain to be the southern Caribbean Sea, opposite to Venezuela and Colombia coasts, but with a larger extension compared with the historical period.

3.2.5. Regional development constraints

The classification of the offshore wind energy resource takes into account factors that are crucial to ensure the present and future viability of the offshore wind energy resource in the Caribbean Sea. This classification, in conjunction with the knowledge of future wind power regime both at annual and seasonal scales, clearly identifies regional differences in the offshore wind energy projections and can help policymakers to adopt and modify strategies for long-term sustainable development in the Caribbean. It is important to have in mind that the present study represents the first step in the development of projects to exploit this resource. Thus, after the current analysis, it is possible to select the most suitable areas for offshore wind energy exploitation in the Caribbean Sea, as well as to know its future viability. However, the later phases of development of offshore wind farms must consider other factors of legal, political, technological or biodiversity conservation nature [44]. The analysis of these aspects should be done on a smaller spatial scale in order to find any possible spatial restriction.

As a first attempt to introduce some of these aspects, the territorial waters and the protected areas of each country and the Caribbean main shipping routes were represented in Figure 11. Territorial waters which includes internal waters, territorial seas up 12 miles and 24 miles from the coast and the Exclusive Economic Zone (EEZ) was represented in Figure 11a attending to the United Nations Convention on the Law of the Sea of 1982 (UNCLOS) and later maritime delimitation treaties between countries. This is an important aspect in the Caribbean Sea due to the high number of islands and archipelagos present in this territory. According to UNCLOS, each country has full sovereignty in their internal waters and their territorial seas up to 12 nautical miles from the coast, purple and green polygons in Figure 11a. In addition, countries have also sovereignty, although more restrictive, to exploit and manage offshore wind farms in the contiguous zone (up to 24 miles) and the EEZ [44].

The marine protected areas (green polygons) according to the United Nations Environment World Conservation Monitoring Centre and the International Union for Conservation of Nature, as well as the main shipping routes in the Caribbean Sea according to the Regional Marine Pollution Emergency Information and Training Center for the Wider Caribbean (REMPEITC-Caribe) [48] were represented in Figure 11b. Marine protected areas may represent a restriction to the installation of offshore wind farms, although it depends on the specific countries' legislation. Regarding the shipping lines, it can be seen that the Panama Canal congregates the main shipping routes in the Caribbean Region (Figure 11b).

Apart from the previously pointed external constraints to the wind resource, other restraints that depend on each country such as fishing, tourism, military uses or the laying of submarine cables and pipelines [44] should also be considered in later steps of the development of offshore wind farms in the Caribbean.

4. Conclusions

Projections of wind speed and power were developed from an ensemble of seven regional climate models from the CORDEX project using the RCP 8.5 greenhouse emission scenario in the Caribbean for the remainder of the 21st century. Then, the future offshore

wind energy resource was classified taking into account wind energy, environmental risk and cost factors and compared with historical data.

The ability of the models to reproduce real wind conditions in the Caribbean was evaluated by means of the overlap between real and modelled data. Results showed that all models reproduced real wind accurately (overlap > 80%) for the period 2009–2016 for all regions of the Caribbean. Taking into account that all models showed a similar level of accuracy, the multi-model mean (which minimizes the bias associated with individual models) was selected to analyze the projections. OP values between multi-model results and buoys were in the order of 90%, showing the reliability of RCMs projected estimations of wind resources in the Caribbean until the end of the 21st century.

Three periods of time were considered for the analysis of changes in wind speed and power projected for the 21st century relative to the historical period: near, mid and far future. All models coincided in a wind increase for the whole Caribbean except in the Yucatán Basin, where a decrease was projected. Both positive and negative trends tended to intensify with time, being highest in the far future, when the maximum percentage of change will be about -6% in the Yucatán Basin and +8% for the rest of the Caribbean.

Changes in wind and wind power were also analyzed at the seasonal scale for the three future periods. There is a consensus between models in the projected increment for the wet season over the entire region, except in the Yucatán Basin, regardless of the period being studied. On the other hand, only a small region in the Venezuela Basin showed a moderate wind increase during the dry season. As previously observed at the annual scale, changes tended to intensify in time, being highest in the far future when the maximum change of wind speed and power are projected to be around 4% and 10% respectively in the dry season, and 10% and 20% in the wet season.

The projected increment during the wet season was associated with changes in the extension of the NASH, which was projected to produce stronger geostrophic winds in the southeastern Caribbean. The moderate increase projected for the southeastern coast of the Caribbean during the dry season was associated with an increment of around 1°C difference between the air temperatures over the land and ocean, intensifying local easterly winds.

The wind energy resource was classified as more than good for most of the Caribbean Sea both for the historical and future period. The extent of richest wind energy resource area, which is opposite to Venezuela and Colombia at present, is projected to increase over the 21st century.

In summary, the high spatial resolution of CORDEX RCMs has shown to be a useful tool for projecting the impact of future climate change on wind power. Near-future, mid-future and far-future projections of wind speed and power density can help policymakers to adopt and modify strategies for long-term sustainable development in the Caribbean. Thus, the followed protocol which includes the classification of offshore wind energy resource and the analysis of its time evolution should be the first step to identify the location of future wind farms. In addition, the later phases of development of offshore wind farms must also consider possible restrictions, such as territorial waters, marine protected areas, shipping lines, fishing, tourism, military uses, etc.

Acknowledgments

Funding: This research was partially supported by Xunta de Galicia under project ED431C 2017/64 “Programa de Consolidación e Estructuración de Unidades de Investigación Competitivas (Grupos de Referencia Competitiva)” co-funded by European Regional Development Fund (FEDER). The Portuguese Science Foundation (FCT) partially supported this research through Postdoctoral grants: SFRH/BPD/97320/2013, SFRH/BPD/118142/2016 and SFRH/BPD/99707/2014 and through the project Pest (C/MAR/LA0017/2013).

Figure Captions

Figure 1. Area under scope and bathymetry. Numbers mark the location of buoys. Blue and red points mark locations where surface air temperature differences between land and sea were calculated.

Figure 2. Weibull PDFs for all buoys (Table 2). Shape parameter (k) and scale parameter (c) are shown in the legend.

Figure 3. Multimodel mean of (a) wind (ms^{-1}), (b) wind power (Wm^{-2}) and their standard deviation (c) and (d), respectively, over the period 2019-2099. STD at each pixel was calculated as $STD = \sqrt{\Sigma|x - \bar{x}|^2/N}$, where x is the value at each pixel and time; $\bar{x}$ is the mean value over the whole period and N is the number of RCMs used.

Figure 4. Multimodel mean of the wind percentage of change for (a) the near future (2019-2045); (b) mid future (2046-2072) and (c) far future (2073-2099) with respect to the historical period (1976–2005). Black dots represent the grid points where a consensus between the different RCMS was obtained.

Figure 5. Multimodel mean of wind (ms^{-1}) for (a) the dry season and (b) the wet season averaged over the period 2019-2099.

Figure 6. Multimodel mean of wind power (Wm^{-2}) for (a) the dry season and (b) the wet season averaged over the period 2019-2099.

Figure 7. Multimodel mean of the wind percentage of change for the dry (left column) and the wet season (right column). (a, b) near future (2019-2045); (c, d) mid future (2046-2072) and (e, f) far future (2073-2099) with respect to the historical period (1976–2005). Black dots represent the grid points where consensus between the different RCMS was obtained.

Figure 8. Multimodel mean of the wind power percentage of change for the dry (left column) and the wet season (right column). (a, b) near future (2019-2045); (c, d) row mid future (2046-2072) and (e, f) far future (2073-2099) with respect to the historical period (1976–2005). Black dots represent the grid points where consensus between the different RCMS was obtained.

Figure 9. Multimodel mean of sea level pressure associated to the NASH during the boreal summer (June-August) for: (a) far future period (2073 to 2099) and (b) historical (1976–2005). Arrows represent geostrophic winds. (c) Geostrophic wind percentage of change in the Caribbean for the far future.

Figure 10. Wind energy classification of the offshore wind energy resource for the Caribbean Sea by means of a CORDEX multi-model ensemble for: (a) historical period 1976–2005, (b) near future (2019-2045), (c) mid future (2046-2072) and (d) far future (2073-2099).

Figure 11. (a) Territorial waters of Caribbean countries according to UNCLOS, which includes internal waters (purple polygons), territorial seas up to 12 miles (green polygons) and 24 miles (orange polygons) from the coast and the Economic Exclusive Zones (red lines). (b) Marine protected areas (green polygons) attending to the United Nations Environment World Conservation Monitoring Centre (UNEP-WCMC) and main shipping lines in the Caribbean Sea according to REMPEITC-Caribe [48].

References:

[1] Zheng C, Pan J. Assessment of the global ocean wind energy resource. Renew Sust Energ Rev 2014; 382-391.

[2] Zheng C, Xia Z, Peng Y, Li, Ch, Du Z. Rezoning global offshore wind energy resources. Renew Energ 2018; 1- 11.

[3] Bingham R D, Agelin-Chaab M, Rosen MA. Feasibility study of a hybrid solar and wind power system for an island community in the Bahamas. Int J Renew Ener Res 2016; 6 (3): 951- 963

[4] Yaw FJr. Cleaner technologies for sustainable tourism: Caribbean case studies. J of Cleaner Prod 2005; 13(2): 117- 134.

[5] Chadee X T, Clarke RM. Wind resources and the levelized cost of wind generated electricity in the Caribbean islands of Trinidad and Tobago. Renew Sustain Energy Rev 2018; 81: 2526- 2540. Doi:10.1016/j.rser.2017.06.059.

[6] Wright RM. Wind energy development in the Caribbean. Renew. Ener 2001; 25: 439-444.

[7] Elliott DL, Aspliden CI, Gowerl GL, Holladay CG, Schwartz MN. Wind energy Resource assessment of the Caribbean and Central America (PNL-6234). Richland, Washington: Pacific Northwest National Laboratory 1987.

[8] Chadee XT, Clarke RM. Large- scale wind energy potential of the Caribbean region using near- surface reanalysis data. Renew Sustain Ener Rev 2014; 30: 45- 58, http://dx.doi.org/10.1016/j.rser.2013.09.018.

[9] Altaii K, Farrugia RN. Wind characteristics on the Caribbean island of Puerto Rico. Renew Ener 2003; 28: 1701- 1710.

[10] Soler- Bientz RS, Watson S, Infield D. Wind characteristics on the Yucatán Peninsula based on short term data from meteorological stations. Ener Conv and Manag 2010; 51: 754- 764.

[11] Chen AA, Daniel AR, Daniel ST, Gray CR. Wind power in Jamaica. Solar Energy 1990 44: 355-365.

[12] Bishop JD, Amaratunga GA. Evaluation of small wind turbines in distributed arrangement as sustainable wind energy option for Barbados. Energy Convers Manage 2008; 49(6): 1652-1661.

[13] Weisser D. A wind energy analysis of Grenada: an estimation using the 'Weibull'density function. Renew Ener 2003; 28(11): 1803-1812.

[14] Soares PM, Lima DC, Cardoso RM, and Coauthors. Western Iberian offshore wind resources: More or less in a global warming climate?. Appl Energy 2017; 203: 72-90.

[15] Moemken J, Reyers M, Feldmann H, and Pinto JG. Future changes of wind speed and wind energy potentials in EURO□CORDEX ensemble simulations. J Geophys Res Atmos 2018.

[16] Staffell I, Pfenninger S. Using bias-corrected reanalysis to simulate current and future wind power output. Energy J 2016; 114; 1224-1239.

[17] Tian Q, Huang G, Hu K, Niyogi D. Observed and global climate model based changes in wind power potential over the Northern Hemisphere during 1979–2016. Energy J 2019; 167; 1224-1235.

[18] Salvação N, Soares CG. Wind resource assessment offshore the Atlantic Iberian coast with the WRF model. Energy J 2018; 145; 276-287.

[19] Pryor SC, Barthelmie RJ, Clausen NE, and Coauthors. Analyses of possible changes in intense and extreme wind speeds over northern Europe under climate change scenarios. Clim Dyn, 2012; **38**: 189–208.

[20] Hueging H, Rabea H, Born K, and Coauthors. Regional changes in wind energy potential over Europe using regional climate model ensemble projections. J Appl Meteorol Climatol 2013; 52: 903–17.

[21] Santos JA, Rochinha C, Liberato MLR, Reyers M, Pinto JC. Projected changes in wind energy potentials over Iberia. Renew Ener 2015; 75: 68-80.

[22] Koletsis I, Kotroni V, Lagouvardos K, Soukissian T. Assessment of offshore wind speed and power potential over the Mediterranean and the Black Seas under future climate changes. Sustain Ener Rev 2016; 60: 234-245.

[23] Davy R, Gnatiuk N, Pettersson L, and Coauthors. Climate change impacts on wind energy potential in the European domain with focus on the Black Sea. Renew Sustain. Ener Rev 2018; 81(2): 1652-1659. doi:10.1016/j.rser.2017.05.253.

[24] Hennemuth TI, Jacob D, Keup-Thiel E, and Coauthors. Guidance for EURO-CORDEX climate projections data use. Available at: https://www.euro-cordex.net/imperia/md/content/csc/cordex/euro-cordex-guidelines-version1.0-2017.08.pdf. Last accessed: 30/09/2018.

[25] Angeles ME, González JE, Erickson III DJ, Hernández JL. The impacts of climate changes on the renewable energy resources in the Caribbean region. J of Solar Ener Engin, 2010; 132: 031009-1- 031009-13.

[26] Yao Z, Xue Z, He R, Bao X, Song, J. Statistical downscaling of IPCC sea surface wind and wind energy predictions for US east coastal ocean, Gulf of Mexico and Caribbean Sea. J Oean U China 2016: 15(4); 577-582.

[27] Monahan AH. The probability distribution of sea surface wind speeds. Part I: theory and sea winds observations. J. Clim. 2006; 19, 497–520.

[28] Monin AS, Obukhov AM. Osnovnye zakonomernosti turbulentnogo peremeshivanija v prizemnom sloe atmosfery (Basic Laws of Turbulent Mixing in the Atmosphere Near the Ground). Trudy geofiz inst, AN SSSR 1954; 24 (151): 163-187

[29] Liu W T, Tang W. Equivalent Neutral Wind, JPL Publication, Jet Propulsion Laboratory, California Institute of Technology Pasadena, California 1996.

[30] Hoogwijk M, De Vries B, Turkenburg W. Assessment of the global and regional geographical, technical and economic potential of onshore wind energy. Ener Econ 2004; 26: 889–919.

[31] Pereira de Lucena AP, Salem Szklo A, Schaeffer R, Marques Dutra R. The vulnerability of wind power to climate change in Brazil. Renew Ener 2010; 35: 904–12.

[32] Drechsel S, Mayr GJ, Messner JW, Stauffer R. Wind speeds at heights crucial for wind energy: measurements and verification of forecasts. J. Appl. Meteor. Climatol 2012; 51(9), 1602-1617.

[33] Engineering Sciences Data Unit. Characteristics of Wind Speed in the Lower Layers of the Atmosphere Near Ground: Strong Winds (Neutral Atmosphere). London, Regent Street, UK: ESDU; 1972.

[34] Hansen FV. Surface Roughness Lengths. Army Research Laboratory 1994.

[35] Holton JR. An introduction to dynamic meteorology 2004. USA: Elsevier.

[36] Sousa MC, Alvarez I, Gomez-Gesteira M, Dias JM. Why coastal upwelling is expected to increase along the western Iberian Peninsula over the next century?. Sci Total Environ 2017; 592, 243-251.

[37] Perkins SE, Pitman AJ, Holbrook NJ, McAneney J. Evaluation of the AR4 Climate Models´ Simulated Daily Maximum temperature, Minimum Temperature, and Precipitation over Australia Using Probability Density Functions. J of Climate 2007; 20:4356- 4376. Doi: 10.1175/JCLI4253.1

[38] Pfeifer S, Bülow K, Gobiet A, Hänsler A, Mudelsee M. Robustness of ensemble climate projections analyzed with climate signal maps: seasonal and extreme precipitation for Germany. Atmosphere 2015; 6(5), 677-698.

[39] Gibbons JD, Chakraborti S. Nonparametric Statistical Inference, fifth ed., Chapman & Hall/CRC Press, Taylor & Francis Group, Boca Raton, FL; 2011.

[40] National Renewable Energy Laboratory (NREL). Wind Energy Resource Atlas of the United States. DOE/CH 10093-10094, October 1986, http://rredc.nrel.gov/wind/pubs/atlas. (Accessed 25 February 2019).

[41] Katsaprakakis DA, Christakis DG. Seawater pumped storage systems and offshore wind parks in islands with low onshore wind potential. A fundamental case study. Energy J 2014; 66: 470-486.

[42] Pierce DW, Barnett TP, Santer BD, Gleckler PJ. Selecting global climate models for regional climate change studies. Proc. Natl. Acad. Sci. U. S. A. 2009; 106, 8441–8446.

[43] Pires AC, Nolasco R, Rocha A, Ramos C, Dubert J,. Climate change in the Iberian Upwelling System: a numerical study using GCM downscaling. Clim Dyn 2015; 47 (1), 451–464.

[44] deCastro M, Costoya X, Salvador S, Carvalho D, Gómez□Gesteira M, Sanz□Larruga F J, Gimeno L. An overview of offshore wind energy resources in Europe under present and future climate. Ann N Y Acad Sci 2018.

[45] Enfield DB, Alfaro EJ. The dependence of Caribbean rainfall on the interaction of the tropical Atlantic and Pacific Oceans. J. Climate 1999; 12: 2093–2103.

[46] Wang C, Lee SK. Atlantic warm pool, Caribbean low level jet, and their potential impact on Atlantic hurricanes. Geophys Res Let 2007; 34: L02703. Doi:10.1029/2006GL028579

[47] Cook K, Vizy E. Hydrodynamics of the Caribbean low level jet and its relationship with precipitation. J Climate 2010; 23: 1477-1494.

[48] Morinière V. Réglain A. Development of a GIS-based database for Maritime Traffic in the Wider Caribbean Region. Strategic Plan, 10-11, 2012. Available at: http://cep.unep.org/racrempeitc/maritime-traffic/Activity%20Report%20GIS-database%20of%20the%20Maritime%20Traffic%20in%20the%20WCR.pdf. Last accessed: 01-04-2019.

Table 1. Regional climate simulations from CORDEX project (http://www.cordex.org) used in this study. Seven GCMs were run with the same RCM (RCA4). The model ID (M_1, …, M_7) will identify the model throughout the rest of the text.

GCMs	ID
NCC-NorESM1-M	M1
MPI-M-MPI-ESM-LR	M2
MIROC-MIROC5	M3
IPSL-IPSL-CM5A-MR	M4
CSIRO-QCCCE-CSIRO-Mk3-6-0	M5
CNRM-CERFACS-CNRM-CM5	M6
CCCma-CanESM2	M7

Table 2. Location of marine buoys distributed in the Caribbean Sea. Buoys were deployed by the National Data Buoy Center (http://www.ndbc.noaa.gov). Numbers correspond to their position in Figure 1.

Number	Buoy	Latitude (ºN)	Longitude (ºW)
1	42056 (Yucatan Basin)	19.918	84.938
2	42057 (Western Caribbean)	16.908	81.422
3	42058 (Central Caribbean)	14.888	74.575
4	42059 (Eastern Caribbean)	12.252	67.51
5	42060 (Caribbean Valley)	16.406	63.188

Table 3. Standard wind speed classification scheme [40].

Class	Annual average wind speed (ms^{-1})	Annual average WPD (Wm^{-2})
1	0 - 4.4	<100
2	4.4 - 5.1	100-150
3	5.1 - 5.6	150-200
4	5.6 - 6	200-250
5	6 - 6.4	250-300
6	6.4 - 7	300-400
7	7 - 9.4	400-1000

Table 4. Normalized criterion used for EWSO, RLO, Cv, Mv, EWS, WD and DC indices related to wind energy factors, environmental risk factors and cost factors.

Normalized value	**EWSO (%)**	**RLO (%)**	**Cv**	**Mv**	**EWS (ms^{-1})**	**WD (m)**	**DC (º)**
0	<20	<20	>1.75	>1.75	>28	>500	>4
0.25	20-40	20-40	[1.25,1.75]	[1.25,1.75]	25-28	100-500	3-4
0.5	40-60	40-60	[0.75,1.25]	[0.75,1.25]	20-25	50-100	2-3
0.75	60-80	60-80	[0.25,0.75]	[0.25,0.75]	15-20	25-50	0.5-2
1	80-100	80-100	<0.25	<0.25	<15	0-25	<0.5

Table 5. Weight coefficient of significant factors in the wind energy classification.

	W_{ann}	EWSO	RLO	Cv	Mv	EWS	WD	DC
Weight	0.22	0.22	0.1	0.1	0.05	0.14	0.07	0.1

Table 6. Classification scheme of wind energy resource.

Class	Categorization value	Resource potential
1	$x \leq 0.4$	Poor
2	$0.4 \leq x \leq 0.5$	Marginal
3	$0.5 \leq x \leq 0.6$	Fair
4	$0.6 \leq x \leq 0.7$	Good
5	$0.7 \leq x \leq 0.8$	Excellent
6	$0.8 \leq x \leq 0.9$	Outstanding
7	$X > 0.9$	Superb

Table 7. Overlap percentage of wind calculated at each buoy and RCM ($OP_{M\#}$) for the period 2009-2016. The last column represents the average of the overlap percentages for the seven RCMs ($<OP>_M$**)**. M is the model skill to reproduce wind offshore and it was calculated as the spatial mean of the overlap percentages for each model. σ is the standard deviation.

Buoy	**OP_{M1}**	**OP_{M2}**	**OP_{M3}**	**OP_{M4}**	**OP_{M5}**	**OP_{M6}**	**OP_{M7}**	**$<OP>_M \pm \sigma$**
1	94.7	95.9	90.5	96.6	94.4	95.7	96.1	**94.8±2.0**
2	95.8	95.6	93.3	94.4	96.9	97.0	81.3	**93.5±5.5**
3	96.8	96.7	99.1	94.8	93.0	86.7	92.8	**94.3±4.0**
4	86.9	91.2	88.8	84.0	94.6	96.4	83.6	**89.4±5.0**
5	87.7	97.9	86.6	85.9	97.6	91.5	84.3	**90.2±5.6**
M	**92.4±4.7**	**95.5±2.5**	**91.7±4.8**	**91.1±5.8**	**95.3±1.9**	**93.5±4.35**	**87.6±6.4**	**92.4±4.9**

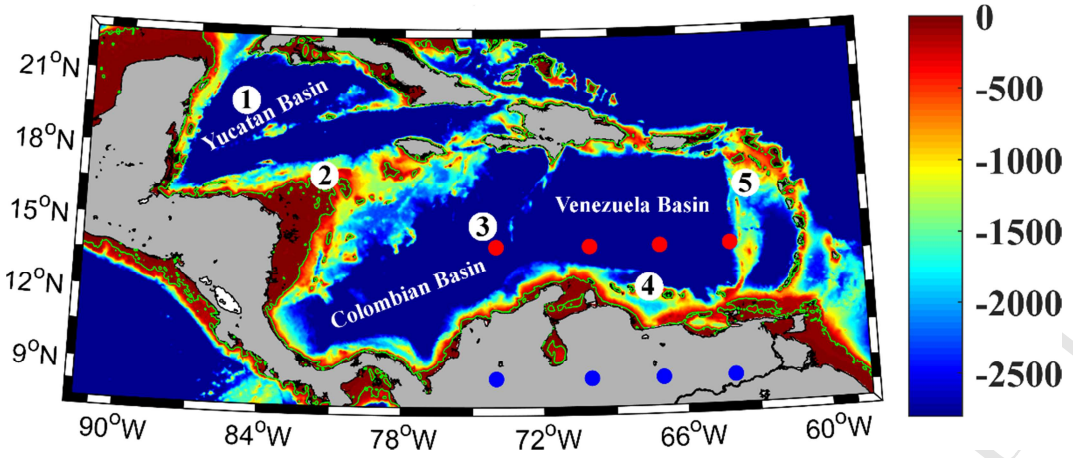

Figure 1. Area under scope and bathymetry. Numbers mark the location of buoys. Blue and red points mark locations where surface air temperature differences between land and sea were calculated.

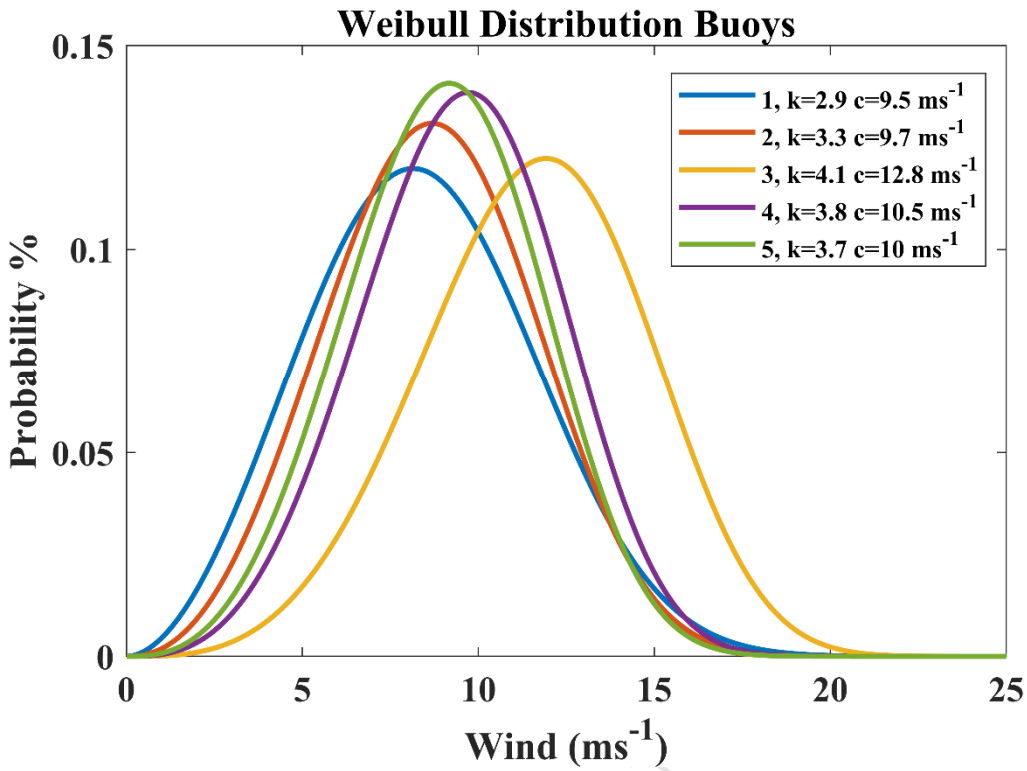

Figure 2. Weibull PDFs for all buoys (Table 2). Shape parameter (k) and scale parameter (c) are shown in the legend.

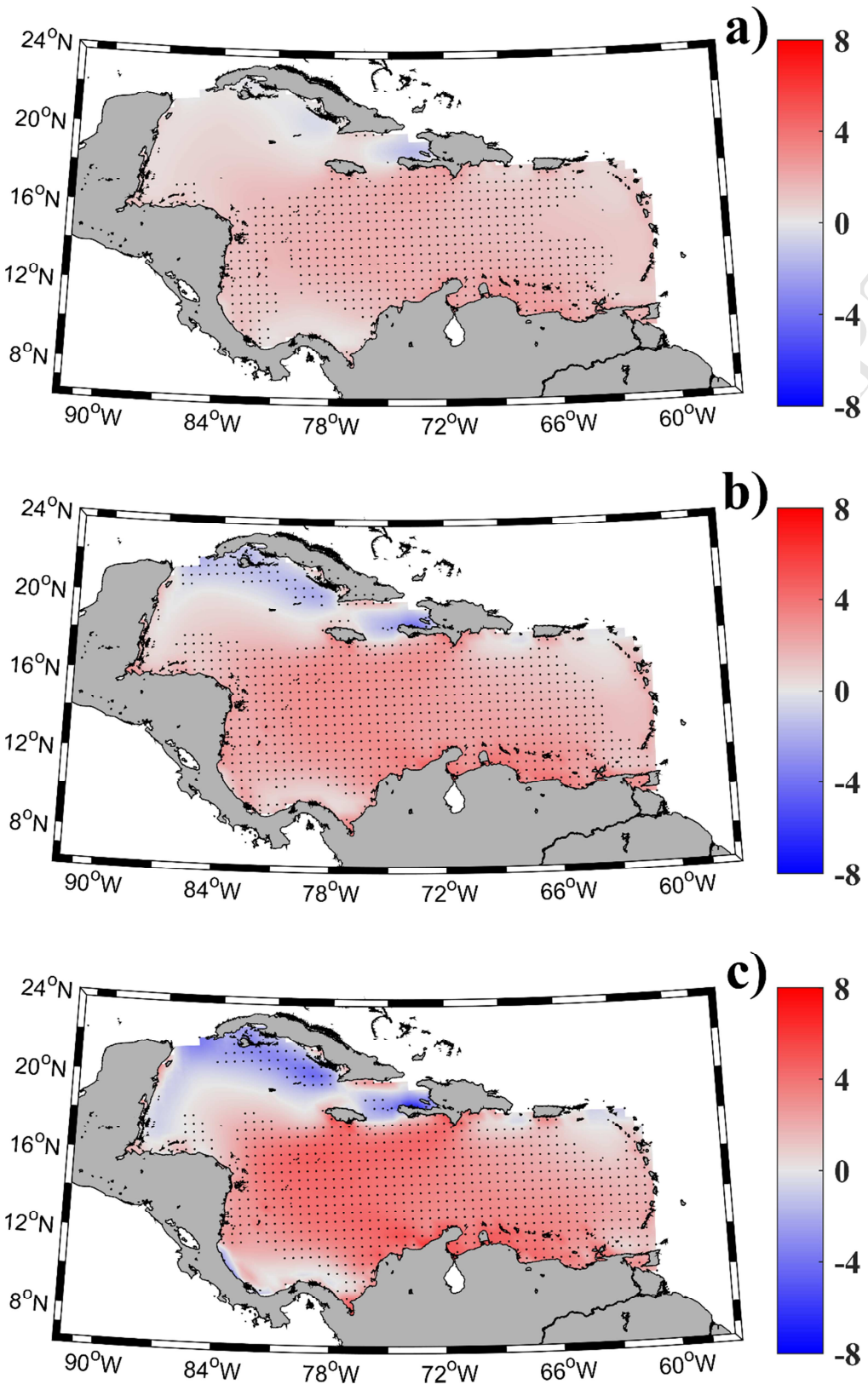

Figure 4. Multimodel mean of the wind percentage of change for (a) the near future (2019-2045); (b) mid future (2046-2072) and (c) far future (2073-2099) with respect to the historical period (1976–2005). Black dots represent the grid points where a consensus between the different RCMS was obtained.

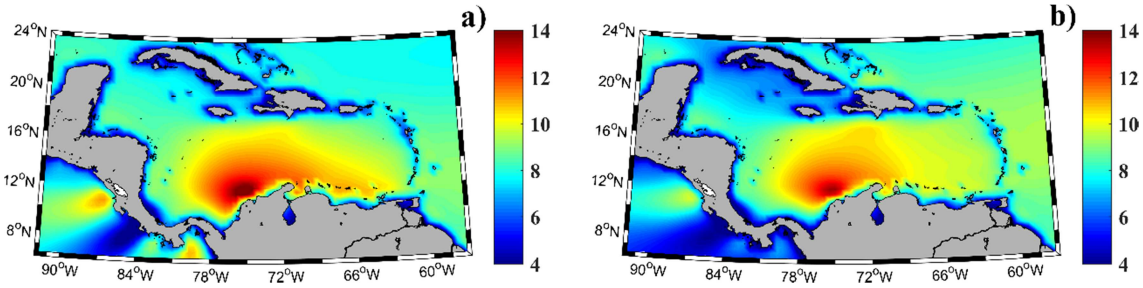

Figure 5. Multimodel mean of wind (ms^{-1}) for (a) the dry season and (b) the wet season averaged over the period 2019-2099.

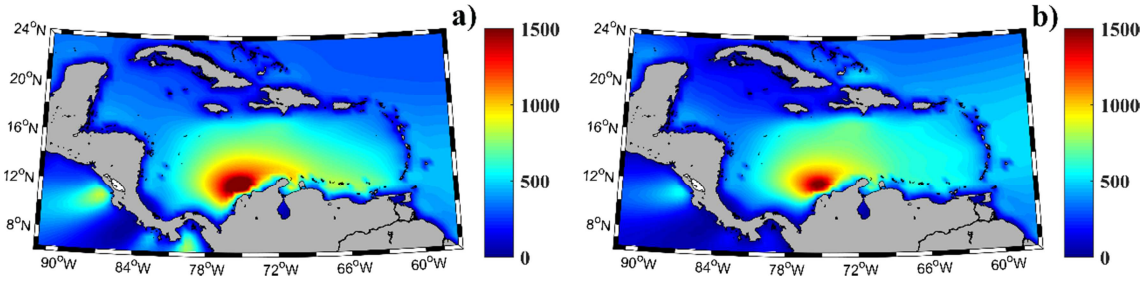

Figure 6. Multimodel mean of wind power (Wm^{-2}) for (a) the dry season and (b) the wet season averaged over the period 2019-2099.

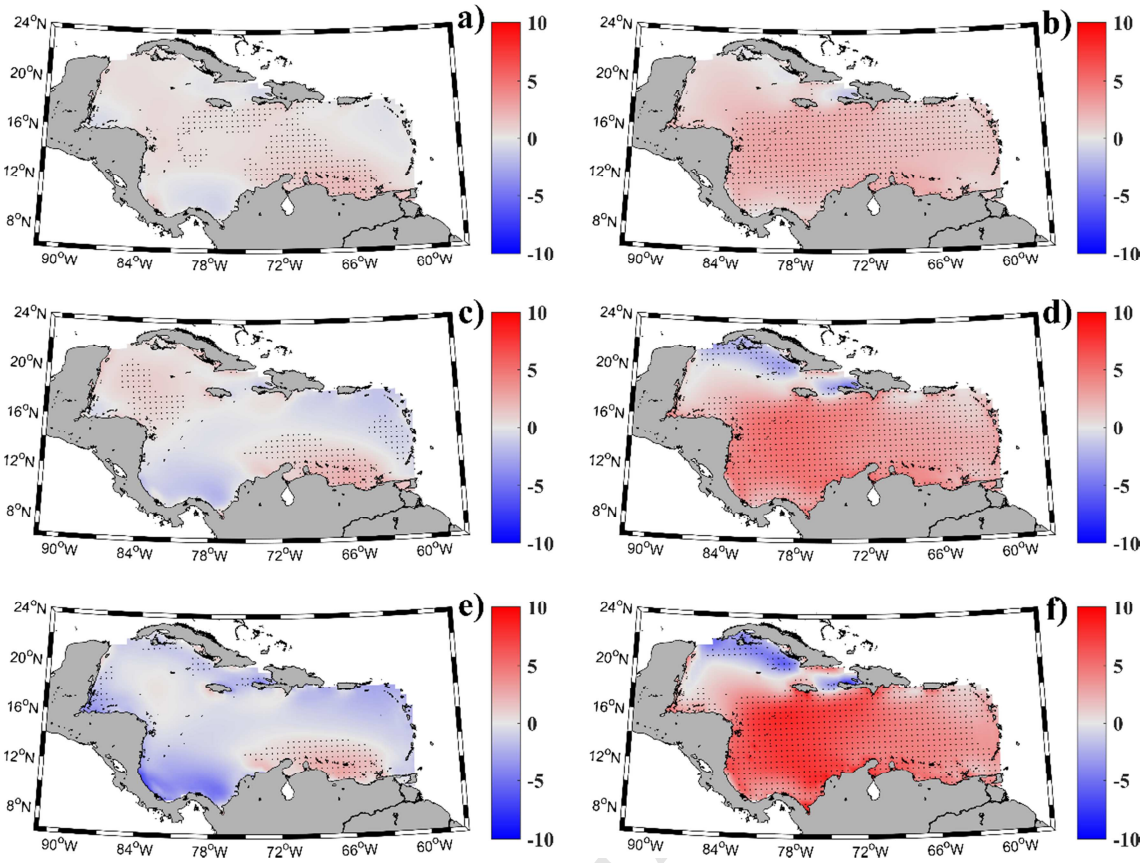

Figure 7. Multimodel mean of the wind percentage of change for the dry (left column) and the wet season (right column). (a, b) near future (2019-2045); (c, d) mid future (2046-2072) and (e, f) far future (2073-2099) with respect to the historical period (1976–2005). Black dots represent the grid points where consensus between the different RCMS was obtained.

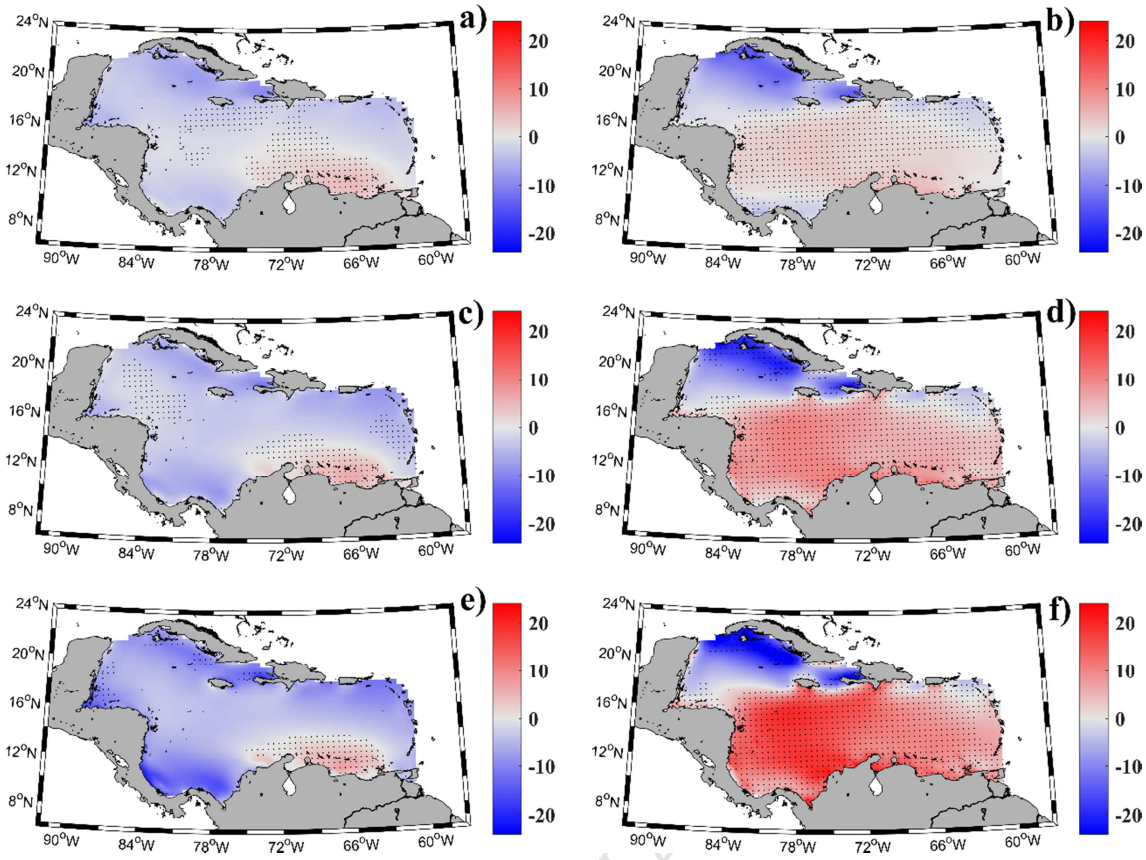

Figure 8. Multimodel mean of the wind power percentage of change for the dry (left column) and the wet season (right column). (a, b) near future (2019-2045); (c, d) row mid future (2046-2072) and (e, f) far future (2073-2099) with respect to the historical period (1976–2005). Black dots represent the grid points where consensus between the different RCMS was obtained.

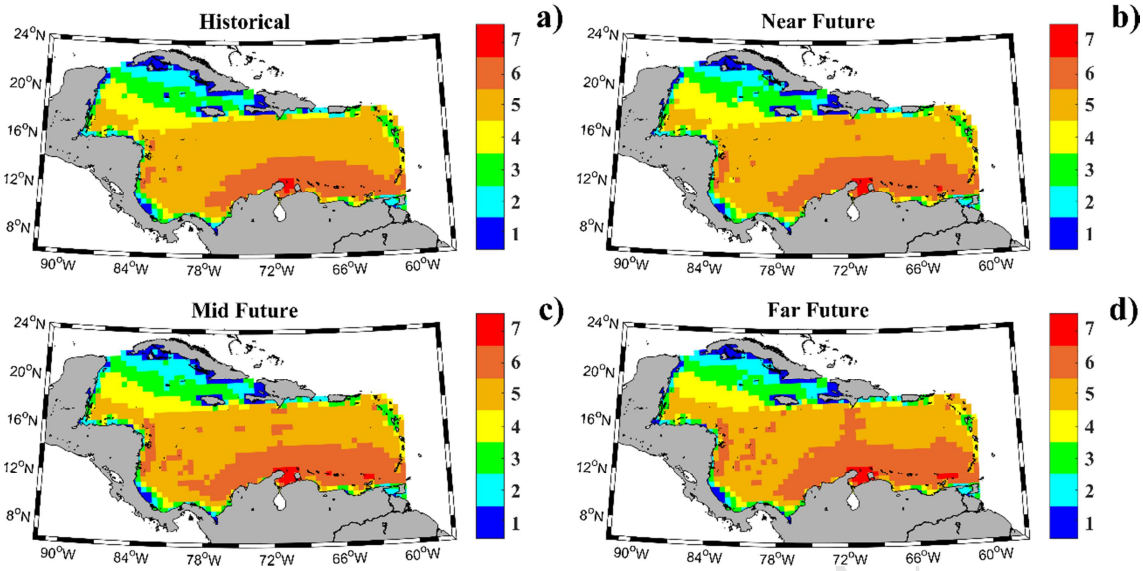

Figure 10. Wind energy classification of the offshore wind energy resource for the Caribbean Sea by means of a CORDEX multi-model ensemble for: (a) historical period 1976–2005, (b) near future (2019-2045), (c) mid future (2046-2072) and (d) far future (2073-2099).

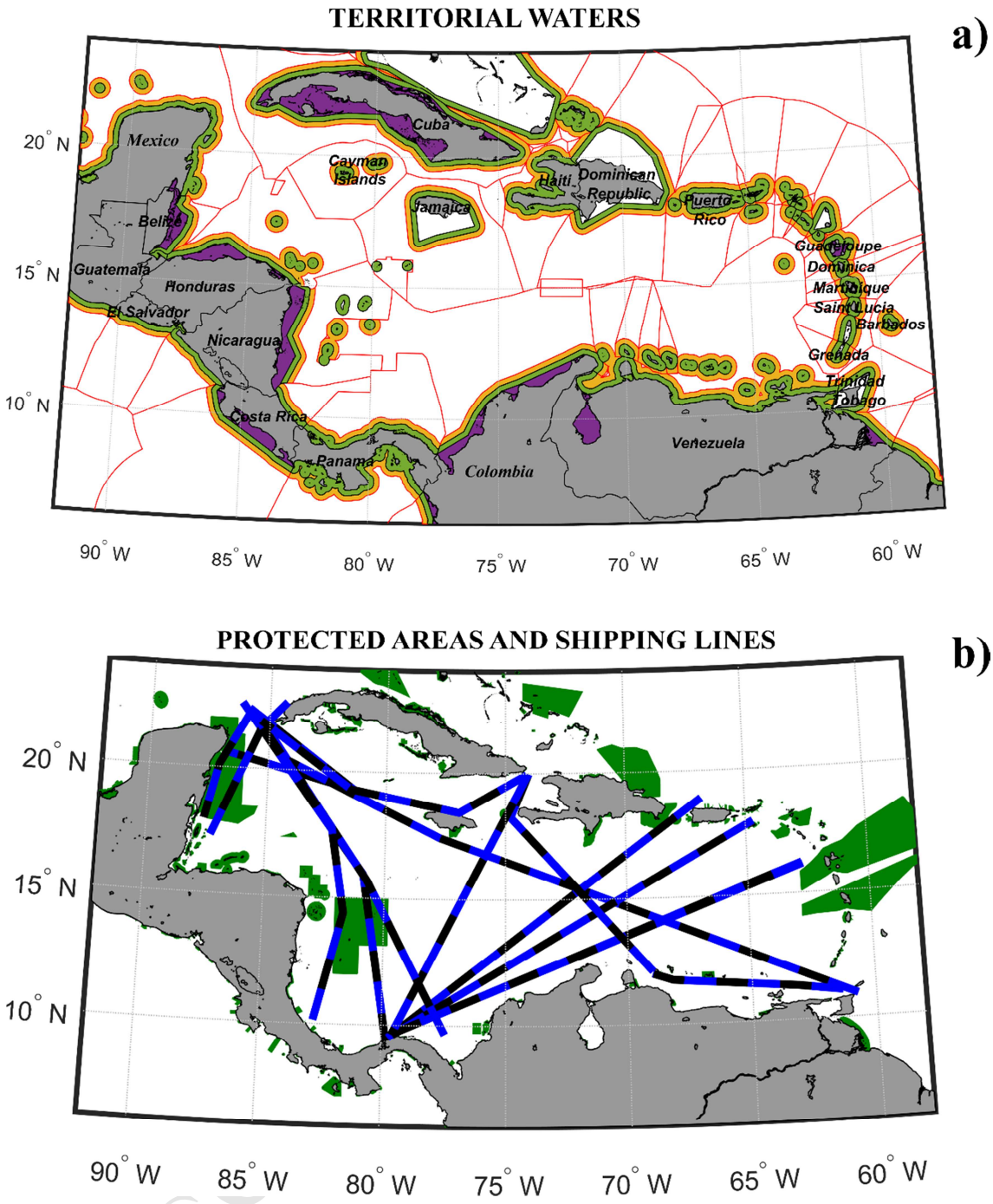

Figure 11. (a) Territorial waters of Caribbean countries according to UNCLOS, which includes internal waters (purple polygons), territorial seas up to 12 miles (green polygons) and 24 miles (orange polygons) from the coast and the Economic Exclusive Zones (red lines). (b) Marine protected areas (green polygons) attending to the United Nations Environment World Conservation Monitoring Centre (UNEP-WCMC) and main shipping lines in the Caribbean Sea according to REMPEITC-Caribe [48].

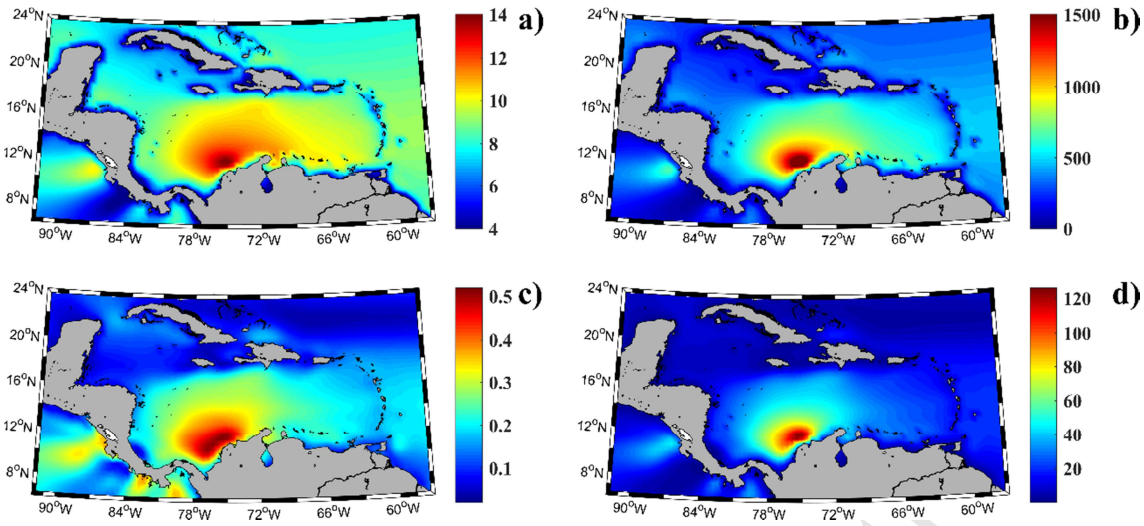

Figure 3. Multimodel mean of (a) wind (ms^{-1}), (b) wind power (Wm^{-2}) and their standard deviation (c) and (d), respectively, over the period 2019-2099. STD at each pixel was calculated as $STD = \sqrt{\Sigma|x - \bar{x}|^2/N}$, where x is the value at each pixel and time; $\bar{x}$ is the mean value over the whole period and N is the number of RCMs used.

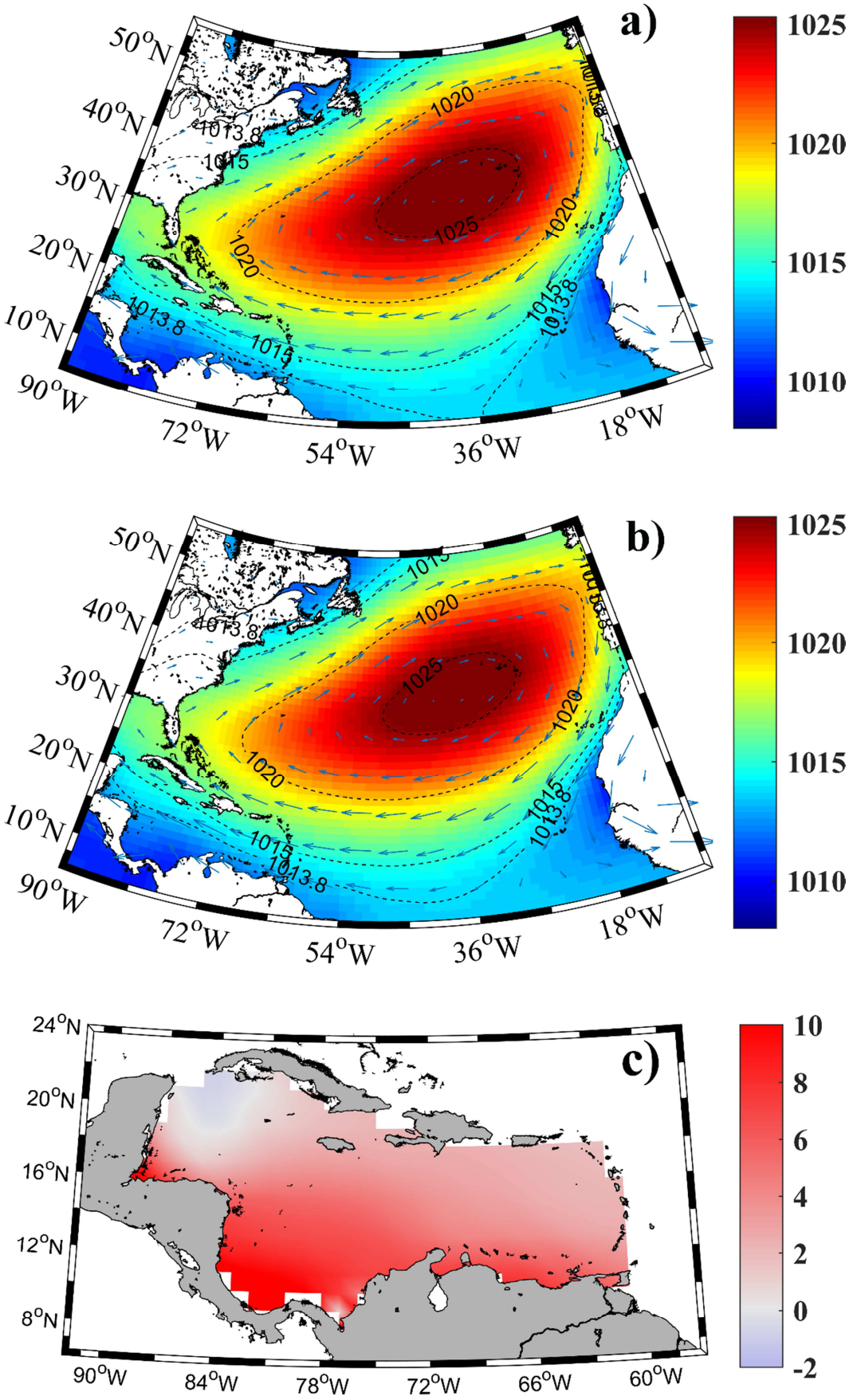

Figure 9. Multimodel mean of sea level pressure associated to the NASH during the boreal summer (June-August) for: (a) far future period (2073 to 2099) and (b) historical

(1976–2005). Arrows represent geostrophic winds. (c) Geostrophic wind percentage of change in the Caribbean for the far future.

Highlights

Influence of climate change on future offshore wind power in the Caribbean

Future projections by means of an ensemble of RCM from the CORDEX under the RCP8.5

Wind increases in most (only in southeastern coast) of Caribbean in wet (dry) season

Wind increase in the wet season associated to changes in the extension of the NASH

Wind increase in dry season due to an increase in land-ocean temperature gradient